THE ASTROPHYSICAL JOURNAL, 538:L7–L11, 2000 July 20

ON-ORBIT PERFORMANCE OF THE *FAR ULTRAVIOLET SPECTROSCOPIC EXPLORER* SATELLITE

D. J. SAHNOW,[1] H. W. MOOS,[1] T. B. AKE,[1,2] J. ANDERSEN,[3] B-G ANDERSSON,[1] M. ANDRE,[1,4] D. ARTIS,[5] A. F. BERMAN,[1] W. P. BLAIR,[1] K. R. BROWNSBERGER,[6] H. M. CALVANI,[1] P. CHAYER,[1,7] S. J. CONARD,[1] P. D. FELDMAN,[1] S. D. FRIEDMAN,[1] A. W. FULLERTON,[1,7] G. A. GAINES,[8] W. C. GAWNE,[3] J. C. GREEN,[6] M. A. GUMMIN,[8] T. B. JENNINGS,[3] J. B. JOYCE,[1] M. E. KAISER,[1] J. W. KRUK,[1] D. J. LINDLER,[9] D. MASSA,[10] E. M. MURPHY,[1] W. R. OEGERLE,[1] R. G. OHL,[1] B. A. ROBERTS,[1] M. L. ROMELFANGER,[1] K. C. ROTH,[1] R. SANKRIT,[1] K. R. SEMBACH,[1] R. L. SHELTON,[1] O. H. W. SIEGMUND,[8] C. J. SILVA,[3] G. SONNEBORN,[11] S. R. VACLAVIK,[3] H. A. WEAVER,[1] AND E. WILKINSON[6]

Received 2000 March 22; accepted 2000 June 12; published 2000 July 14

ABSTRACT

The launch of the *Far Ultraviolet Spectroscopic Explorer* (*FUSE*) has been followed by an extensive period of calibration and characterization as part of the preparation for normal satellite operations. Major tasks carried out during this period include the initial coalignment, focusing, and characterization of the four instrument channels and a preliminary measurement of the resolution and throughput performance of the instrument. We describe the results from this test program and present preliminary estimates of the on-orbit performance of the *FUSE* satellite based on a combination of these data and prelaunch laboratory measurements.

Subject headings: instrumentation: spectrographs — space vehicles — ultraviolet: general

1. INTRODUCTION

The *Far Ultraviolet Spectroscopic Explorer* (*FUSE*) is obtaining high-resolution, far-ultraviolet spectra of faint astronomical objects in the 905–1187 Å wavelength range (Moos et al. 2000). Details of the *FUSE* design and the predicted performance based on preflight measurements have been given previously (Friedman et al. 1999; Sahnow et al. 1996). After an initial period of spacecraft checkout and on-orbit guidance tests, the two far-ultraviolet detectors were powered on in 1999 August, and several months of checkout and science verification activities began. This included evaluation of the overall satellite performance and preliminary instrument characterization. Science operations began in 1999 October, but characterization activity will continue throughout the 3 yr mission with decreasing frequency. Results from these early investigations show that the satellite is, with a few exceptions, performing quite well; most measures show that the performance is at or near preflight predictions and is adequate to meet the goals of the mission.

The *FUSE* design consists of four coaligned optical channels, two of which have optics coated with SiC (SiC1 and SiC2) and two coated with LiF over Al (LiF1 and LiF2). Each channel is made up of a telescope primary mirror, a Focal Plane Assembly containing the spectrograph entrance apertures, a holographically ruled diffraction grating, and a portion of a detector. The previous Letter (Moos et al. 2000) presents an overview of the *FUSE* mission, including the scientific background and an overall description of the instrument. This Letter discusses the measured performance of the *FUSE* satellite as of 2000 February, with an emphasis on the properties of the instrument that affect the scientific data.

2. DETECTOR PERFORMANCE

2.1. *Design*

The two *FUSE* detectors have been described previously (Siegmund et al. 1997; Sahnow et al. 2000). Each detector has two microchannel plate (MCP) segments with a helical double delay line (DDL) anode. The front surface of each of the four segments is coated with a KBr photocathode to obtain quantum efficiencies of 14%–30% across the *FUSE* bandpass, depending on the segment and the wavelength. The detectors are windowless, but in order to preserve the photocathode the microchannel plate and anode assemblies were enclosed inside a vacuum box for ground testing and calibration. On-orbit, a mechanical door was opened once the spectrograph cavity pressure reached an acceptably low level. High-voltage operations of the two detectors began on 1999 August 13 and 26.

The size and location of pixels in DDL detectors are not fixed but are determined by timing and analog measurements. Temperature changes can therefore cause geometric shifts and distortions in the detector, which must be accounted for in the data processing. In order to characterize these changes, electronic stimulation pulses are introduced into the preamplifiers of the electronics during the recording of spectra and flat fields. These stimulation pulses are injected into the position readout anode, where they are processed through the entire readout electronics chain. In this way, image effects due to temperature variations in the anode and electronics can be accurately tracked. The nominal size of the *FUSE* detector pixels is 6 μm in x, and 9–16 μm in y, depending on the segment.

[1] Department of Physics and Astronomy, Johns Hopkins University, 3400 North Charles Street, Baltimore, MD 21218.
[2] Computer Sciences Corporation, 1100 West Street, Laurel, MD 20707.
[3] Honeywell Technology Solutions, Inc., Columbia, MD 21045.
[4] Institut d'Astrophysique de Paris, INSU CNRS, 98 bis Boulevard Arago, F-75014 Paris, France.
[5] Johns Hopkins University Applied Physics Laboratory, 11100 John Hopkins Road, Laurel, MD 20723.
[6] Center for Astrophysics and Space Astronomy, University of Colorado, Campus Box 389, Boulder, CO 80309.
[7] Primary affiliation: Department of Physics and Astronomy, University of Victoria, P.O. Box 3055, Victoria, BC V8W 3P6, Canada.
[8] Space Sciences Laboratory, University of California, Berkeley, Berkeley, CA 94720.
[9] Advanced Computer Concepts, Inc., Code 681, NASA Goddard Space Flight Center, Greenbelt, MD 20771.
[10] Raytheon Information Technology and Scientific Services, Code 681, NASA Goddard Space Flight Center, Greenbelt, MD 20771.
[11] Laboratory for Astronomy and Solar Physics, Code 681, NASA Goddard Space Flight Center, Greenbelt, MD 20771.

2.2. *Flat-Field and Signal-to-Noise Ratios*

After photon statistics, the most important source of noise in the data is pixel-to-pixel variations and other features in the detector response. Long flat-field exposures obtained on the ground contain 40–100 photon events per pixel. Since a spectral resolution element of 0.04 Å represents a sum over ~6 *x*-pixels and ~7–70 *y*-pixels (depending on the astigmatic height of the spectrum), they can support signal-to-noise ratios of 50–120. However, variations in the thermal conditions during these exposures may make them unsuitable for on-orbit use. Lower signal-to-noise ratio flat fields have been obtained on-orbit with an onboard stimulation lamp; they are used to monitor any gross changes in detector response.

The ground-based flats showed a complex structure from blocked pores and other MCP defects. The pixel-to-pixel response also shows a moiré-fringe–like quasi-periodic variation with an ~50 μm scale caused by the slightly different geometric scales between the front, middle, and rear MCP plates in the stack (Tremsin et al. 1999). These features also appear in the on-orbit flats, to the limits of the signal-to-noise ratios of these measurements, although a careful comparison requires taking account of the differences in temperature between the ground measurements and the on-orbit data.

An alternative method for minimizing the effects of fixed pattern noise in the data is to dither the spectrum by moving it back and forth in the dispersion direction on the detector. Using this technique, a given wavelength falls on different detector pixels; the addition of the coaligned spectra then averages out the fixed pattern noise. Observations of G191-B2B acquired by employing this strategy recovered signal-to-noise ratios of ~120 per spectral resolution element in one-dimensional spectra, consistent with photon statistics (see Fig. 1).

2.3. *Background*

The background, from a combination of radioactivity in the MCPs (Siegmund, Vallerga, & Wargelin 1988), cosmic rays, other high-energy particles, and scattered airglow, is approximately 0.8 counts cm^{-2} s^{-1} on all four segments at night; no hot spots are seen. Before launch, when the particle background was not present, typical rates were ~0.35 counts cm^{-2} s^{-1}. Because there is no shutter on the *FUSE* instrument, the detectors are constantly collecting photons, primarily from airglow when there is no target in the apertures. This contamination means it is not possible to get an accurate background measurement from the detectors in the region where the spectra fall. Thus, unused regions of the detector are used to measure the intrinsic detector background. Since there appears to be no identifiable structure to the background, no spatial variation has been assumed.

Although scattered light from the target is small (Moos et al. 2000), stray light is present at several levels. A vertical "stripe" of enhanced counts is present on one detector segment; its intensity varies with the Lyβ airglow, so it is thought to be caused by light entering the spectrograph from an unknown location. In addition, scattered light causes an increase in the background by a factor of 2–3 for observations made during the day. These effects are at a level such that they affect data for only the lowest flux targets. Finally, weak scattered solar emission lines have been identified in the SiC-channel spectra during the sunlit portion of the orbit at some pointing orientations.

For observations where minimizing the detector background is more important than maximizing the number of photons collected, detector pulse-height thresholds can be applied to the data to further decrease the background to ~0.5 counts cm^{-2} s^{-1} or less. Data are taken on board with very limited pulse-height thresholding, but upper and lower thresholds can be applied during the processing of the photon list data in order to exclude more of the background, if appropriate.

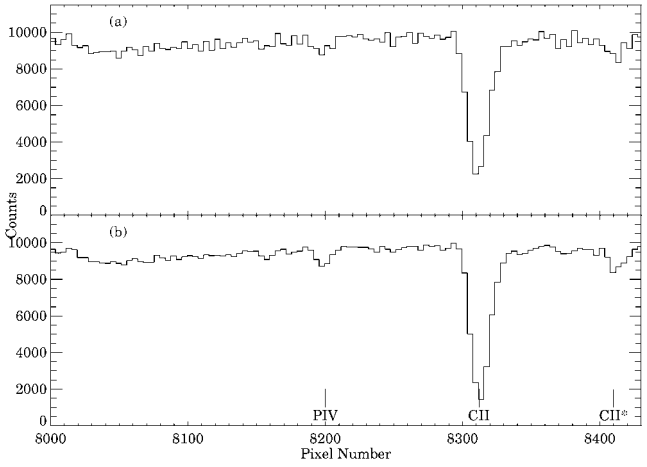

FIG. 1.—Portion of the spectrum of G191-B2B, binned by 4, which includes spectral features from C II λ1036.34, C II* λ1037.02, and P IV λ1035.52. Shown in (*a*) is an undithered spectrum, with a signal-to-noise ratio of ~63 per spectrograph resolution element (6 pixels), while (*b*) displays a dithered spectrum with a signal-to-noise ratio of ~120 per spectrograph resolution element. The high-frequency fixed pattern noise in the upper figure is significantly reduced by dithering, so that the signal-to-noise ratio predicted by photon statistics is nearly recovered.

2.4. *Flux Limitations*

FUSE was designed to observe faint objects. As a result of its high sensitivity, it is difficult to observe objects as bright as those observed by *Copernicus*. In fact, the bright limit of 1×10^{-10} ergs cm^{-2} s^{-1} Å^{-1} established in order to ensure the long-term health of the detectors precludes observing any of the *Copernicus* targets by several orders of magnitude. In addition, the data system was not designed for high count rates (≥32,000 counts s^{-1}). Bright emission line objects present a different problem since they can easily deplete the charge from the MCPs in local regions, which could lead to a permanent loss of sensitivity at those wavelengths. In addition, the intrinsic dead time of the detector electronics limits a single detector segment to a count rate of ~33,000 counts s^{-1}. Higher flux targets could be observed, but they would have such low efficiency that the detector lifetime would be unduly compromised for a limited benefit.

Variations in detector gain with time are being monitored as part of the normal characterization program. It is expected that as the mission progresses, the gain will drop, and the high voltage will be raised to compensate for the decreased gain.

2.5. *Single-Event Upsets*

The only significant detector anomaly discovered on-orbit was the sensitivity of the electronics to single-event upsets (SEUs). When the detector electronics were powered on for the first time several days after launch, the detector data processing unit began reporting errors in the memory that stores the code controlling the detector. Further investigation revealed that the memory was being corrupted by high-energy particles as the satellite passed through the South Atlantic Anomaly

(SAA). These SEUs, which now occur roughly once every 3 days on each detector, have no effect on the scientific data but are a potential detector health and safety issue since corruption of the executing code could cause unpredictable behavior. Although it is not possible to decrease their frequency (and, in fact, the approaching solar maximum may cause it to increase), their effect has been minimized by developing a procedure by which the instrument flight computer reloads the corrupted detector code whenever an SEU is detected. Rarely, about once per month, a potentially more vital part of the memory is corrupted, causing the detector to reboot and turn off the detector high voltage as a safety measure. This currently requires ramping up the high voltage via ground commands, which typically results in a 1 day loss of data for that detector; this process is now being automated to reduce the loss of observing time.

3. MECHANICAL PERFORMANCE

To compensate for expected changes of alignment in orbit, mechanisms to adjust the mirrors and Focal Plane Assemblies (FPAs) containing the spectrograph entrance apertures were built into the *FUSE* design. A carbon-fiber structure with an extremely low coefficient of thermal expansion and athermal optical mounts were used to minimize mechanical variations that might affect the ability to hold the optics stable to several microns over a several meter distance.

On-orbit measurements have shown that thermal motions are larger than expected, causing small rotations of both the gratings and the mirrors. The rotation of the gratings causes the spectra to move in two dimensions on the detectors in a roughly sinusoidal fashion over the course of an orbit; if uncorrected, this smears the spectra by up to 0.09 Å, depending on the channel. This motion is correlated with the pointing of the satellite and appears to be Earth-driven. Algorithms have been developed to minimize these shifts during the pipeline processing of the data. At present, these corrections decrease the amplitude of the motion to less than 0.015 Å. Additional studies are underway with the goal of improving this further.

The mirror rotation, which makes it difficult to keep the four channels coaligned, initially resulted in a misalignment large enough for targets to drift out of the large ($30'' \times 30''$) aperture in one or more channels in many instances. Since that time, we have empirically mapped its behavior and limited the frequency of this occurrence to less than ~10% of observations. In addition, a theory exists for the cause of this motion. An understanding of the drift in more detail is now being obtained in preparation for making regular observations in the smaller apertures.

A number of workarounds were developed for these problems. These are primarily operational constraints imposed in order to control the thermal variations seen by certain parts of the satellite. Characterization is not complete, but it is believed that with the development of thermal models and careful scheduling of observations, this can be improved in the future, allowing reasonable efficiency in the $30'' \times 30''$ and $4'' \times 20''$ apertures.

4. OPTICAL PERFORMANCE

The optimal optical performance of *FUSE* depends on a narrow point-spread function (PSF) from the telescopes and thus good slit transmission, proper coalignment of the four channels, and a focused optical system. The focus problem for each channel can be divided into two parts: location of the optimal position of the FPA in order to obtain the best spectrograph focus and a proper telescope mirror to FPA distance in order to maximize slit transmission. The FPAs contain three apertures for general observing: a $30'' \times 30''$ aperture (LWRS) through which most observations have been made thus far, an intermediate $4'' \times 20''$ (MDRS) slit, and a narrow $1\farcs25 \times 20''$ slit (HIRS) aperture.

4.1. *Telescope Performance*

The telescopes provide a complex, nonuniform point-spread function at the FPAs. Preflight measurements and analysis of a spare mirror, combined with metrology on the flight mirrors, showed that 88% ± 5% of the encircled energy is within a $1\farcs5$ diameter circle at 1000 Å (Ohl et al. 2000a). In-flight, knife-edge scans made using the FPAs showed that the telescope PSFs are consistent with these ground measurements, with FWHMs of $\leq 1\farcs1$–$1\farcs7$, depending on the channel (Ohl et al. 2000b). This narrow PSF means that the spectral resolution of point-source objects is not limited by the FPA apertures but by the mechanical stability factors described above; the ~$0\farcs3$ satellite pointing stability also has a negligible effect.

The knife-edge scans mentioned above were also used to optimize the mirror to FPA distances, which have been located to ± 50 μm.

4.2. *Co-alignment*

Coarse alignment of the *FUSE* channels is achieved by adjusting the telescope mirrors; this is required infrequently. In the MDRS and HIRS apertures, fine alignment is accomplished using the FPAs, by slewing the satellite, measuring the signal in all four channels as a function of position, and adjusting the FPA positions to maximize throughput. In the LWRS aperture, these peakups are not necessary.

The ability to maintain coalignment of the four channels is dependent on knowledge of the thermal and mechanical stability of the system, which affects the rotation of the telescope mirrors. Because of the mechanical instabilities, observations in all but the LWRS aperture require multiple peakups per orbit in order to maintain a reasonable throughput. In the LWRS aperture, where coalignment is much less critical, a satisfactory alignment can typically be maintained for weeks without interruption. This requires only small adjustments of the FPAs and mirrors as long as satellite pointing angle constraints are followed.

4.3. *Spectrograph Resolution and Instrument Focus*

The aberrations from a standard spherical grating ruled with regularly spaced grooves would result in a point source being imaged to a line many millimeters tall on the detector. The holographic corrections in the *FUSE* optical design (Grange 1992; Green et al. 1994) significantly reduce the vertical extent of these images; they range from ~200 to ~900 μm for a point source, depending on wavelength. One of the astigmatic correction points, where the height is minimized, was chosen to be at O VI λ1032 for the LiF channels, in order to limit the background contribution at this astrophysically important line. The two correction points in the SiC channels are near the edges of the bandpass, in order to limit the height over as much of the spectrum as possible and thus minimize the detector background. This size is significant compared with the vertical extent of the entrance apertures (220–330 μm), so that little or no spatial information is available from the instrument, and then only at wavelengths near the correction points.

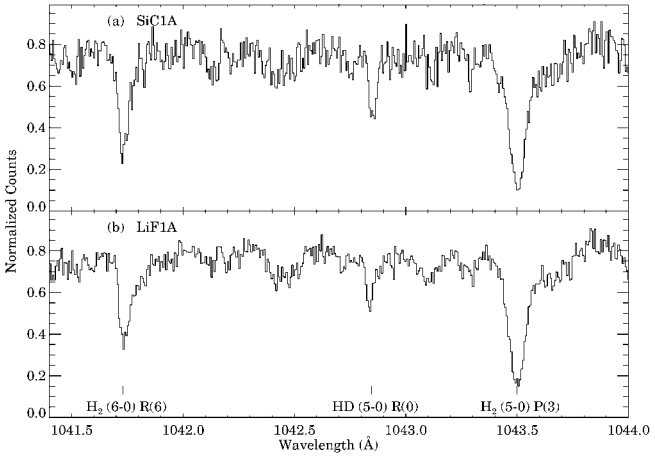

FIG. 2.—Spectrum of the line of sight toward WD 0439+466 showing the (6–0) *R*(6) and (5–0) *P*(3) transitions of H_2, and the (5–0) *R*(0) line of HD in the SiC1 and LiF1 channels. The HD line shows a resolving power of ~13 km s^{-1}. The unidentified features are probable stellar absorption features.

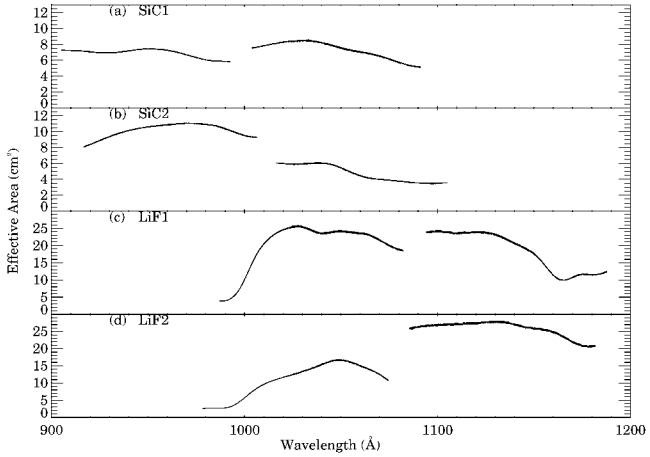

FIG. 3.—Estimated effective area of the four channels of the *FUSE* instrument, based on measurements of white dwarfs and model spectra. Due to variations in coating reflectivity, grating efficiency, and detector sensitivity, there is a substantial variation between channels. Errors are typically ~10%, except above 1150 Å. Note that the scales are different for the SiC and LiF channels.

A consequence of the holographic correction is that the spectra include significant curvature due to astigmatism and that the line width varies as a function of wavelength. As part of the processing that occurs in the science data pipeline, this curvature must be removed in order to achieve the highest resolving power. At wavelengths away from a correction point, there is a trade-off between the amount of light included (i.e., the vertical extent of the spectrum used in the analysis) and the resulting resolving power. The standard pipeline extraction includes close to 100% of light, but smaller extraction windows can be used to obtain narrower line spread functions at many wavelengths, although at the price of lower throughput.

The velocity resolution, $c\Delta\lambda/\lambda$, of the *FUSE* spectrographs has been determined by measuring the widths of absorption features in the spectra of astrophysical objects. Figure 2 shows a plot in the 1041–1044 Å region of the line of sight to WD 0439+466 that has been used to measure resolution. Since *FUSE* is limited to observing faint objects, the velocity structure along the line of sight to these objects is often complex, which can significantly broaden the lines. Thus, these measurements represent an upper limit to the instrument resolution. Measurements with the spectrograph focus settings at the launch values showed upper limits to the velocity resolutions of ~20 km s^{-1}, and values of this order are appropriate for the interpretation of data presented in the accompanying Letters. Starting in 1999 December, adjustments were made to the instrument to optimize the resolving power. Those changes have improved the SiC channels to ~17 km s^{-1} and the LiF channels to ~13 km s^{-1} in the LWRS. Changes in resolution as a function of wavelength, which are on the order of 10%, are caused by both the optical design and variations of the intrinsic detector PSF with position (typically ~25 μm in the dispersion direction). Before launch, measurements made using a H_2 source showed marginally better resolution (Wilkinson et al. 1998; Cha, Sahnow, & Moos 1999). Additional adjustments are planned in order to improve these values further.

On-orbit, the positions of only the primary mirrors and the FPAs can be adjusted. In the LWRS aperture, where most of the early observations have been made, the focus of the instrument is determined solely by the position of the mirrors, and the resolution is limited by the telescope PSF, the satellite pointing stability, and the mirror and grating stability. Observations in the smaller apertures, where the positions of the FPAs are important, have begun as our understanding of the thermally induced mirror motions has progressed.

The highest possible resolution will require use of the narrowest apertures, but this will likely result in a significant loss of throughput, particularly in the SiC channels.

5. ON-ORBIT CALIBRATION

5.1. *Sensitivity*

Observations of hot DA white dwarfs have been used by previous missions to obtain a photometric calibration in this spectral region (Davidsen et al. 1992; Kruk et al. 1995, 1997, 1999; Hurwitz et al. 1998). The preliminary *FUSE* sensitivity calibration used for early data analysis was derived by two means: comparison of an observation of the hot DA white dwarf WD 2211−495 with a synthetic spectrum and comparison of an observation of CSPN K1-16 with a spectrum from the Hopkins Ultraviolet Telescope. The synthetic spectrum of WD 2211−495 was computed by D. Finley, using the model code of D. Koester, with an effective temperature of 64,000 K, $\log g = 7.4$, and normalized to $V = 11.77$ (Finley et al. 1997). Better characterized DA white dwarfs (G191-B2B, HZ 43, and GD 246) became observable later in the mission, which allowed a more accurate determination of the effective area. The current estimate of the effective area, based primarily on these stars, is shown in Figure 3 for each of the channels as a function of wavelength. It is comparable to preflight estimates.

As part of our regular calibration program, we will return to these calibration targets roughly once per month in order to monitor the expected decrease in effective area due to contamination and exposure to atomic oxygen (Moos et al. 2000). Early indications are that this drop is less than expected.

An optical anomaly, due to the astigmatism in the system and a wire mesh in front of the detector, is present in the data and can reduce the throughput over particular wavelength intervals. The effect is visible in all channels but is most apparent in LiF1 above 1150 Å (see Fig. 3), where it can reduce the flux by up to 40%. Typically, however, the impact is much less. The position and severity depend on observational pa-

rameters, such as the placement of the star in the slit. After further characterization, the flux calibration will be modified to account for this feature.

5.2. *Wavelength Calibration*

The *FUSE* instrument uses astrophysical sources for wavelength calibration. Therefore, the absolute wavelength determination requires a comparison of spectra with *Hubble Space Telescope* and ground-based data. During spectrograph integration and testing, H_2 spectra were used to map the wavelength scale, which is highly nonlinear because of the variation in size of the analog detector pixels with position (Cha, Sahnow, & Moos 1999). The dispersion is 6.2–6.7 mÅ pixel^{-1}, depending on the segment, with local variations of a few percent over most of the detector. High-order polynomials were developed to describe this distortion to approximately a spectrograph resolution element, which was expected to remain stable, aside from the expected stretches and shifts caused by variations in detector temperature. A combination of downward-looking airglow and astronomical sources was planned to tie the ground-based solution to the in-flight data. However, these corrections have not yet been fully implemented, limiting the accuracy of the preliminary wavelength solution. It is generally better than 0.1 Å with some larger excursions. Activities currently underway will substantially improve this.

6. EVENT BURSTS

An unexplained feature observed in the data is the intermittent increase in the count rate from an as yet undetermined source. The pulse-height distributions of these "event bursts" are consistent with the distributions exhibited by photons, so they are apparently due to light rather than particles or some other source internal to the detector. Their spatial distribution on the detector, however, does not match that of the spectra. The source of these events is unknown.

These bursts have durations that range from a few to several hundred seconds and have maximum intensities that are typically 20,000 s^{-1}. Attempts to correlate their occurrence with orbital location, ram vector, or other orbital phenomena have been unsuccessful, although they occur primarily in orbital morning, with many occurring near noon. Early in the mission, while the satellite was pointed in the continuous viewing zone in order to avoid observing the bright Earth, they occurred on nearly every orbit. The frequency has dropped significantly since that time, but it is unclear if that is an effect of changes in pointing geometry, due to constraints provided by the mirror and grating motions or to some other effect, such as a lower pressure in the spectrograph cavity.

Since the bursts are isolated in time—rarely occurring more than once per orbit—they can easily be screened from time tag data during ground processing without a significant loss of observing efficiency; a pipeline module to automatically remove these times from the data is currently under development. It is not possible to remove them from spectral image data, but since these observations typically have much higher count rates, the bursts provide much less contamination.

7. SUMMARY

The *Far Ultraviolet Spectroscopic Explorer* is performing well on-orbit; early characterization activity is now complete, and routine scientific observations have begun. We have presented the first results from the characterization program, which will continue throughout the mission. Despite several as yet unexplained anomalies, high-quality data addressing a wide variety of scientific problems is being collected, as seen in the accompanying Letters.

We gratefully acknowledge the many people who have contributed to the success of the *FUSE* mission during its design, construction, and characterization. This work is based on data obtained by the NASA-CNES-CSA *FUSE* mission operated by Johns Hopkins University. Financial support to US participants has been provided by NASA contract NAS5-32985.

REFERENCES

Cha, A. N., Sahnow, D. J., & Moos, H. W. 1999, Proc. SPIE, 3765, 495
Davidsen, A. F., et al. 1992, ApJ, 392, 264
Finley, D. S., Koester, D., & Basri, G. 1997, ApJ, 488, 375
Friedman, S. D., et al. 1999, Proc. SPIE, 3765, 460
Grange, R. 1992, Appl. Opt., 31, 3744
Green, J. C., Wilkinson, E., & Friedman, S. D. 1994, Proc. SPIE, 2283, 12
Hurwitz, M., et al. 1998, ApJ, 500, L1
Kruk, J. W., Brown, T. M., Davidsen, A. F., Espey, B. R., Finley, D. S., & Kriss, G. A. 1999, ApJS, 122, 299
Kruk, J. W., Durrance, S. T., Kriss, G. A., Davidsen, A. F., Blair, W. P., Espey, B. R., & Finley, D. S. 1995, ApJ, 454, L1
Kruk, J. W., Kimble, R. A., Buss, R. H., Jr., Davidsen, A. F., Durrance, S. T., Finley, D. S., Holberg, J. B., & Kriss, G. A. 1997, ApJ, 482, 546
Moos, H. W., et al. 2000, ApJ, 538, L1
Ohl, R. G., Saha, T. T., Friedman, S. D., Barkhouser, R. H., & Moos, H. W. 2000a, Appl. Opt., in press
Ohl, R. G., et al. 2000b, Proc. SPIE, in press
Sahnow, D. J., Friedman, S. D., Oegerle, W. R., Moos, H. W., Green, J. C., & Siegmund, O. H. W. 1996, Proc. SPIE, 2807, 2
Sahnow, D. J., et al. 2000, Proc. SPIE, in press
Siegmund, O. H. W., Vallerga, J., & Wargelin, B. 1988, Proc. IEEE, 35, 524
Siegmund, O. H. W., et al. 1997, Proc. SPIE, 3114, 283
Tremsin, A. S., Siegmund, O. H. W., Gummin, M. A., Jelinsky, P. N., & Stock, J. M. 1999, Appl. Opt., 38, 2240
Wilkinson, E., Green, J. C., Osterman, S. N., Brownsberger, K. R., & Sahnow, D. J. 1998, Proc. SPIE, 3356, 18